Draft version 0.2

ATLAS NOTE

June 22, 2013

Studies of Vector Boson Scattering And Triboson Production with an Upgraded ATLAS Detector at a High-Luminosity LHC

The ATLAS Collaboration

Abstract

The Phase 2 upgrade of the ATLAS detector would greatly increase the sensitivity to an extended electroweak symmetry-breaking sector beyond the Standard Model Higgs mechanism. A common feature of such an extended sector is the enhancement of vector boson scattering at high energy. Sensitivity to new physics is also gained through probing Quartic Gauge Boson Couplings via triboson production. Using detector performance parameterizations, we present the expected gain in sensitivity for ATLAS datasets with an integrated luminosity of 300 fb^{-1} and 3000 fb^{-1} at a center-of-mass energy of 14 TeV.

1 Introduction

The exploration of physics at the TeV scale is the primary goal of the LHC, and the luminosity upgrade of the LHC can have a major impact in discovering an extended electroweak symmetry-breaking sector beyond the Standard Model (SM) Higgs mechanism.

Following the discovery of massive W and Z bosons, a reason for expecting new particles or interactions at the TeV energy scale has been the prediction that an untamed rise of the vector boson scattering (VBS) cross section in the longitudinal mode would violate unitarity at this scale. In the SM it is the Higgs particle which is responsible for maintainting unitarity in this process. It is important to confirm this effect experimentally. Other mechanisms for enhancing vector boson scattering at high energy are possible, even after the existence of the SM Higgs boson is established.

A striking experimental feature of vector boson scattering is the presence of two high-p_T jets in the forward regions, similar to those found in Higgs production via vector boson fusion. The absence of color exchange in the hard scattering process leads to a rapidity gap in the central part of the detector; however the gap topology may be difficult to exploit due to the high level of pileup at a high-luminosity LHC.

The non-abelian nature of the electroweak sector predicts the self-interaction of electroweak gauge bosons in the form of triple and quartic gauge boson couplings (TGC and QGC). Whilst the study of these couplings offers an important test of the SM, QGCs are additionally connected to the electroweak symmetry breaking sector, together with the Higgs boson, to ensure unitarity at high energies for scattering processes. QGCs therefore offer a new window on the electroweak symmetry-breaking mechanism and a probe for new physics, not extensively explored in previous experiments. Triboson production is directly sensitive to QGCs and its study is therefore complementary to VBS studies. Even though triboson production cross sections are smaller than diboson ones, QGCs can be sensitive to new processes that leave the TGC sector unchanged; for example, the exchange of additional heavy bosons generates tree-level contributions to QGCs while contributions to TGCs only occur at the one-loop level and are thus suppressed [1].

We present four studies of sensitivity to beyond-SM (BSM) scenarios for four final states: VBS for WZ production in the tri-lepton channel, VBS for ZZ production in the four-lepton channel, VBS for WW production in the same-sign dilepton channel, and $Z\gamma\gamma$ triboson production in the dilepton plus diphoton channel. Triggering on these channels is relatively straightforward with dilepton triggers.

2 Higher Dimension Operators

The SM Lagrangian contains dimension-4 operators. New physics can be parameterized in terms of higher-dimension operators in an effective field theory. Multi-boson production is modified by certain dimension-6 and dimension-8 operators containing the Higgs and/or gauge boson fields. We study the effects of new physics parameterized by $\mathrm{SU}(2)_L{\times}\mathrm{U}(1)_Y$ gauge-invariant, CP-even operators in these categories.

In particular, we focus on the coefficient $c_{\phi W}/\Lambda^2$ [2], which is associated with a dimension-6 operator, as well as f_{S0}/Λ^4, f_{T1}/Λ^4, f_{T8}/Λ^4 and f_{T9}/Λ^4 [3], which are coefficients associated with dimension-8 operators. Here Λ is a mass-dimensioned parameter associated with the new physics.

The $c_{\phi W}$ parameter is of interest because it affects the Higgs boson coupling to electroweak gauge bosons and hence triboson production and vector boson scattering (VBS), but it does not affect diboson production. Therefore, previous studies at LEP and the Tevatron using diboson production would not constrain this operator. If the Higgs couplings to gauge bosons were found to deviate from the SM values, it would be very interesting to check if such an operator would produce compatible signals in triboson production and vector boson scattering. Furthermore, while we have chosen the operator associated

with $c_{\phi W}$ to illustrate this complementarity between vector boson scattering and Higgs boson coupling measurements, there is another dimension-6 operator with the same characteristics but involving the B gauge field. Differentiating between these operators using the combination of triboson production, vector boson scattering and Higgs coupling measurements would be a very interesting program of exploration of non-SM couplings in the gauge-Higgs sector.

The f_{S0} parameter is studied as its associated linear operator can be related to the non-linear operator with coefficient a_4 in the Electroweak Chiral Lagrangian, which has been probed in previous studies [4]. The f_{S0} dimension-8 operator again involves gauge and Higgs fields but with different gauge and tensor structure and dimensionality as compared to dimension-6 operator discussed above. We will illustrate the differences in kinematic distributions induced by this operator in vector boson scattering, demonstrating the ability to probe deeper into the gauge-Higgs interaction with such studies.

Finally, the f_{Tn} set of coefficients are associated with dimension-8 operators only involving the gauge fields and therefore do not directly affect the Higgs boson couplings. Their gauge and tensor structure are again different from the other operators discussed above, potentially yielding further differentiation power using rates and kinematics of triboson production and VBS. None of the dimension-8 operators can affect diboson production and are therefore unconstrained by previous studies at LEP and the Tevatron. They are uniquely studied in triboson production and VBS at the LHC.

The higher-dimension operators ultimately violate unitarity at sufficiently high energy since they represent an approximation of the underlying UV-safe BSM theory by expanding in inverse mass dimension. For individual studies we have checked the unitarity bounds [5, 6, 7] and study events within the kinematic range where unitarity is satisfied.

3 Monte Carlo Simulation

SM and BSM predictions were generated using Monte Carlo (MC) techniques. Events were simulated using the Madgraph generator [8]. Leading-order cross sections are used; ignoring the QCD k-factor leads to conservative estimates of the sensitivity. Particle showers were simulated using Pythia version 6.426 [9]. The leading-order PDF set CTEQ6L1 is used [10]. Outgoing truth-level electrons, photons, and hadrons were clustered into anti-k_{T} jets with $R = 0.4$ [11] unless otherwise noted.

The sensitivity to new physics in vector boson scattering and triboson production depends on jet, lepton and missing energy reconstruction in the high-pileup regime. Fully simulated events under high-pileup conditions have been produced, and efficiencies and resolutions have been estimated for the various objects. These parameterizations of detector performance have been used to smear particle-level outputs for various new-physics scenarios [12].

4 VBS $ZZ \to \ell\ell\ell\ell$

In this channel, the following new analysis has been performed since the European Strategy Submission, based on the dimension-6 operator

$$\mathcal{L}_{\phi W} = \frac{c_{\phi W}}{\Lambda^2}\mathrm{Tr}(W^{\mu\nu}W_{\mu\nu})\phi^{\dagger}\phi \tag{1}$$

The fully-leptonic $ZZjj \to \ell\ell\ell\ell jj$ channel has a small cross section but provides a clean, fully reconstructible ZZ final state. A forward jet-jet mass requirement of 1 TeV reduces the contribution from jets accompanying non-VBS diboson production.

4.1 Monte Carlo Predictions

MadGraph 1.4.2 [8] was used to generate the non-VBS background where ZZ production is accompanied by initial-state radiation of two jets. SM and non-SM ZZ production via VBS were simulated using MadGraph 1.5.9. In both cases Z bosons were required to decay to electron or muon pairs.

4.2 Event Selection

Events are considered VBS ZZ candidates provided they meet the following criteria:

- Exactly four selected leptons (each with $p_T > 25$ GeV) which can be separated into two opposite sign, same flavor pairs (No Z mass window requirement)
- At least one selected lepton must fire the trigger.
- At least two selected jets, each with $p_T > 50$ GeV
- $m_{jj} > 1$ TeV, where m_{jj} is the invariant mass of the two highest-p_T selected jets

4.3 Statistical Analysis

In order to determine the expected sensitivity to BSM ZZ contribution, the background-only p_0-value expected for signal+background is calculated using the $m_{4\ell}$ spectrum. Figure 1 shows the reconstructed 4-lepton invariant mass distribution, and signal significance as a function of $c_{\phi W}/\Lambda^2$. In Table 1 the 5σ

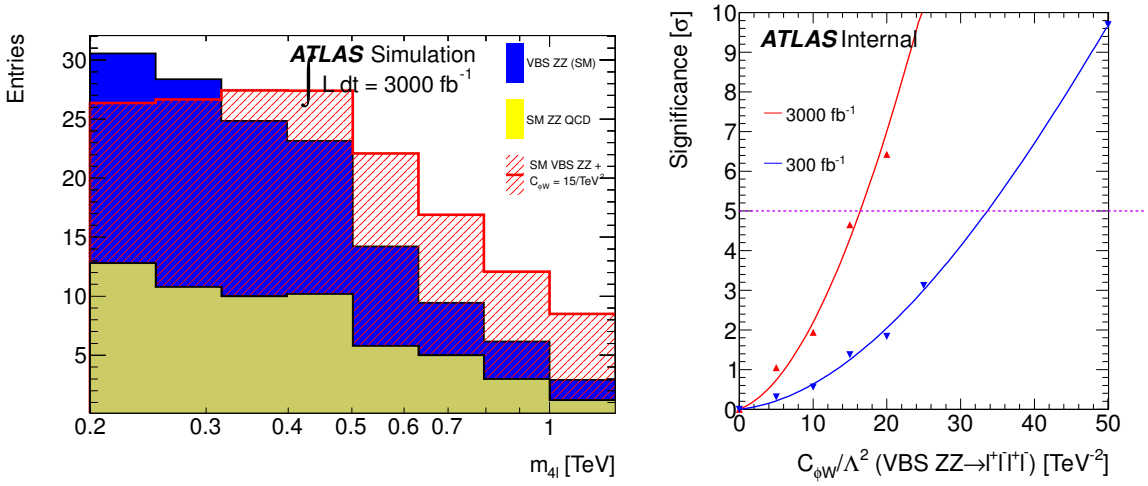

Figure 1: In the $pp \to ZZ + 2j \to \ell\ell\ell\ell + 2j$ process, the reconstructed 4-lepton mass ($m_{4\ell}$) spectrum is shown after requiring $m_{jj} > 1$ TeV (left), and signal significance as a function of $c_{\phi W}/\Lambda^2$ (right). *** ATLAS INTERNAL ***

discovery potential is illustrated, showing the improvement possible with the increased luminosity.

	$300\ \text{fb}^{-1}$	$3000\ \text{fb}^{-1}$
$c_{\phi W}/\Lambda^2$	$32\ \text{TeV}^{-2}$	$16\ \text{TeV}^{-2}$

Table 1: Summary of expected sensitivity to anomalous VBS $ZZ \to 4\ell$ signal at $\sqrt{s} = 14$ TeV, quoted in the terms of 5σ-significance discovery values of $c_{\phi W}/\Lambda^2$.

5 VBS $WZ \to \ell\nu\ell\ell$

This analysis is new since the European Strategy Submission. We parameterize new physics in this channel using the operator

$$\mathcal{L}_{T,1} = \frac{f_{T1}}{\Lambda^4}\mathrm{Tr}[\hat{W}_{\alpha\nu}\hat{W}^{\mu\beta}] \times \mathrm{Tr}[\hat{W}_{\mu\beta}\hat{W}^{\alpha\nu}] \quad (2)$$

The fully leptonic $WZjj \to \ell\nu\ell\ell jj$ channel has a larger cross section than $ZZjj \to \ell\ell\ell\ell jj$ and can still be reconstructed by solving for the neutrino p_z using the W boson mass constraint.

In order to use the W mass constraint, the lepton from W decay must first be identified. If two lepton flavors occur in an event, the unpaired lepton is assumed to come from the W boson. If all three leptons have the same flavor, the invariant masses of all combinations of opposite-sign pairs are calculated, and the pair whose mass is closest to the Z mass is called the Z pair; the unpaired lepton is then used in the neutrino p_z determination.

In the event that there are multiple neutrino p_z solutions to the W mass constraint equation, the solution with the smallest magnitude is chosen. If no real p_z solution exists, the $E_{\mathrm{T}}^{\mathrm{miss}}$ is varied minimally to give a unique solution.

Figure 2 shows the reconstructed 4-lepton invariant mass distribution for this channel.

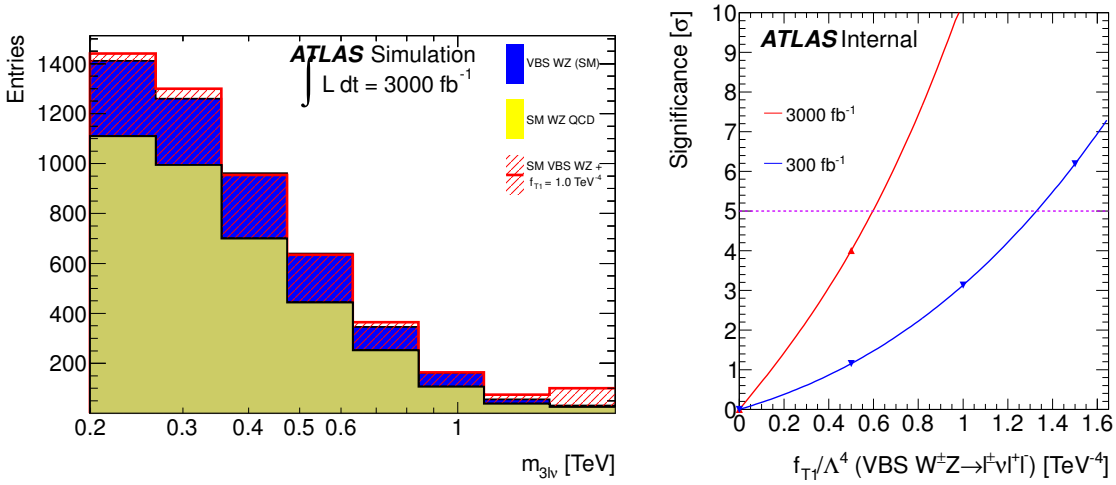

Figure 2: In the $pp \to WZ + 2j \to \ell\nu\ell\ell + 2j$ channel, the reconstructed WZ mass spectrum using the charged leptons and the neutrino solution after requiring $m_{jj} > 1$ TeV (left), and and signal significance as a function of f_{T1}/Λ^4 (right). *** ATLAS INTERNAL ***

5.1 Monte Carlo Predictions

Non-VBS WZ production in association with initial-state radiation of two jets was simulated using MadGraph [8]. MadGraph 1.5.9 was used to generate SM and non-SM VBS WZ production. Each W boson was required to decay to an electron and neutrino or a muon and neutrino, and each Z boson was required to decay to an electron or muon pair.

5.2 Event Selection

Events are considered VBS WZ candidates provided they meet the following criteria:

- Exactly three selected leptons (each with $p_T > 25$ GeV) which can be separated into an opposite sign, same flavor pair and an additional single lepton
- At least one selected lepton must fire the trigger.
- At least two selected jets with $p_T > 50$ GeV.
- $m_{jj} > 1$ TeV, where m_{jj} is the invariant mass of the two highest-p_T selected jets

5.3 Statistical Analysis

The statistical analysis is identical to that employed in Sec. 4.3. Figure 2 shows the signal significance as a function of f_{T1}/Λ^4. In Table 2 the 5σ discovery potential is illustrated, showing the improvement possible with the increased luminosity.

	$300\,\text{fb}^{-1}$	$3000\,\text{fb}^{-1}$
f_{T1}/Λ^4	$1.3\ \text{TeV}^{-4}$	$0.6\ \text{TeV}^{-4}$

Table 2: Summary of expected sensitivity to anomalous VBS WZ signal at $\sqrt{s} = 14$ TeV, quoted in the terms of 5σ-significance discovery values of f_{T1}/Λ^4.

6 VBS $W^\pm W^\pm \to \ell^\pm \nu \ell^\pm \nu$

The potential for new physics via dimension-8 gauge-invariant operators is presented in the scattering of same-sign W bosons (ssWW). The dimension-8 operator

$$\mathcal{L}_{S,0} = \frac{f_{S0}}{\Lambda^4}[(D_\mu \phi)^\dagger D_\nu \phi)] \times [(D^\mu \phi)^\dagger D^\nu \phi)] \tag{3}$$

is chosen to parameterize the new physics in terms of the magnitude of the coefficient f_{S0}/Λ^4. This analysis is new since the European Strategy submission [13].

The two leading jets are used to tag the vector boson scattering process $pp \to W^\pm W^\pm + 2j \to l^\pm \nu l^\pm \nu + 2j$ where l is electron or muon. The same-sign dilepton channel is relatively free of mis-identification backgrounds from W+jets and QCD multi-jet processes, as well as $t\bar{t}$ production. We protect against pile-up jets by requiring the tagging jets to have $p_T > 50$ GeV.

6.1 Monte Carlo Predictions

The signal samples were generated using MadGraph version 1.5.10. Cross sections calculated by MadGraph were found to be in agreement with VBFNLO calculations within 2% for the SM VBS process and within 10% for non-zero values of f_{S0}/Λ^4.

The main background contributions are from $WZjj$, $W\gamma$, jets faking leptons, lepton charge flips, and the QCD diagrams of ssWW. The WZ, $W\gamma$, and ssWW-QCD backgrounds were generated using MadGraph version 1.5.9. The misidentified-lepton, photon-conversion (from $W\gamma$ production) and charge-flip contributions were accounted for by scaling the WZ background by a conservative factor of ≈ 2 taken from the study of ssWW with current ATLAS data.

model	300 fb^{-1}	3 ab^{-1}
f_{S0}/Λ^4	11 TeV^{-4}	5 TeV^{-4}

Table 3: Summary of 5σ discovery values of f_{S0} using the $pp \to W^{\pm}W^{\pm} + 2j \to \ell^{\pm}\nu\ell^{\pm}\nu + 2j$ search in the VBS mode at pp collision center-of-mass energy of 14 TeV.

6.2 Event Selection

Events are considered ssWW candidates provided they meet the following criteria:

- Exactly two selected leptons (each with $p_T > 25$ GeV) with the same charge.
- At least one selected lepton must fire the trigger.
- At least two selected jets with $p_T > 50$ GeV.
- $m_{jj} > 1$ TeV, where m_{jj} is the invariant mass of the two highest-p_T selected jets

6.3 Statistical Analysis

The statistical analysis is performed by constructing templates of the m_{lljj} distribution for different values of f_{S0}/Λ^4. The template for QCD and mis-identification backgrounds is included. Here m_{lljj} is the 4-body invariant mass of the two leading leptons and the two leading jets in the event, which we found to be a robust and sensitive variable since calculating the true WW invariant mass is not possible when two neutrinos are present. The distribution of m_{lljj} and the signal significance as a function of f_{S0}/Λ^4 are shown in Fig. 3.

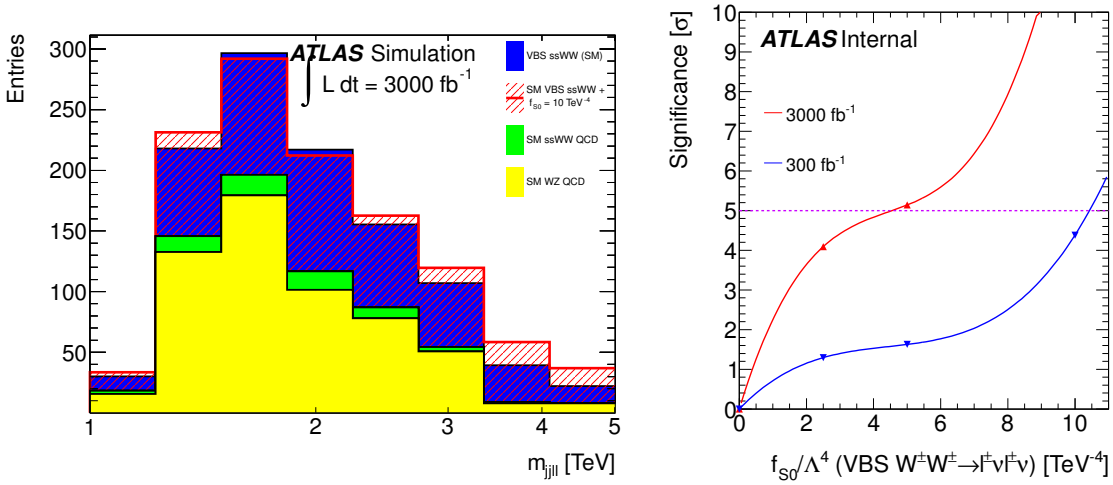

Figure 3: The reconstructed 4-body mass spectrum using the two leading leptons and jets (left) and the signal significance (in standard deviations) as a function of f_{S0} using the same-sign $WW \to \ell\nu\ell\nu$ VBS channel at pp center-of-mass collision energy of 14 TeV. *** ATLAS INTERNAL ***

7 $Z\gamma\gamma$ in the dilepton plus diphoton channel

The $Z\gamma\gamma$ mass spectrum at high mass is sensitive to BSM triboson contributions. The lepton-photon channel allows full reconstruction of the final state and calculate the $Z\gamma\gamma$ invariant mass. This analysis

is new since the European Strategy Submission. We parameterize the BSM physics using the following operators

$$\begin{aligned} \mathcal{L}_{T,8} &= \frac{f_{T8}}{\Lambda^4} B_{\mu\nu}B^{\mu\nu}B_{\alpha\beta}B^{\alpha\beta} \\ \mathcal{L}_{T,9} &= \frac{f_{T9}}{\Lambda^4} B_{\alpha\mu}B^{\mu\beta}B_{\beta\nu}B^{\nu\alpha} \end{aligned} \quad (4)$$

7.1 Monte Carlo Predictions

MadGraph 1.5.10 [8] was used to generate all $Z\gamma\gamma$ samples and background samples, $Z\gamma j$ and Zjj. In both cases Z bosons were required to decay to electron or muon pairs. After Pythia 6 parton showering, the reconstruction effects of resolution and identification efficiency are applied using Delphes [14] with the ATLAS parametrizations. A constant jet-to-photon fake rate of 10^{-3} is applied to each jet in the $Z\gamma j$ and Zjj samples to construct smooth background templates.

7.2 Event Selection

Events are considered $Z\gamma\gamma$ candiates provided they meet the following criteria:

- $p_T(l) > 25$ GeV, $|\eta(l)| < 2.0$
- $p_T(\gamma) > 25$ GeV, $|\eta(\gamma)| < 2.0$
- At least one lepton and one γ with $p_T > 160$ GeV
- $|m_{ll} - 91\ \text{GeV}| < 10$ GeV
- $\Delta(l,\gamma) > 0.4$
- $\Delta(l,l) > 0.4$

The 160 GeV transverse momentum requirement on one lepton and one photon can improve the sensitivity of aQGC. The 10 GeV invariant mass window cuts around Z boson mass peak can suppresses the $\gamma*$ contribution to the dilepton. The large angle cut between photon and lepton and the high transverse-momentum requirement of the photon reduces the FSR contribution. This leads to the phase space which is uniquely sensitive to the QGC. Figure 4 (left) shows the reconstructed 4-body invariant mass distribution for this channel. Figure 4 (right) shows the enhancement of the yield in the tail of the photon p_T distribution due to anomalous QGC.

7.3 Statistical Analysis

The distribution of $m_{Z\gamma\gamma}$ is used for hypotheses testing by comparing the sum of the SM and background processes to the BSM templates (including backgrounds) obtained from the dimension-8 operators in Eqn. 4. The dominant process in the QGC-sensitive kinematic phase space is the true $Z\gamma\gamma$ production while the fake background $Z\gamma j$ and Zjj are subdominant.

The statistical analysis is identical to that employed in Sec. 4.3. Figure 5 shows the expected signal significance as a function of BSM physics parameters. Quoted in Table 4 are the 5σ-significance discovery values and 95% C.I. of the coefficients for an integrated luminosity of $300\,\text{fb}^{-1}$ and $3000\,\text{fb}^{-1}$ respectively.

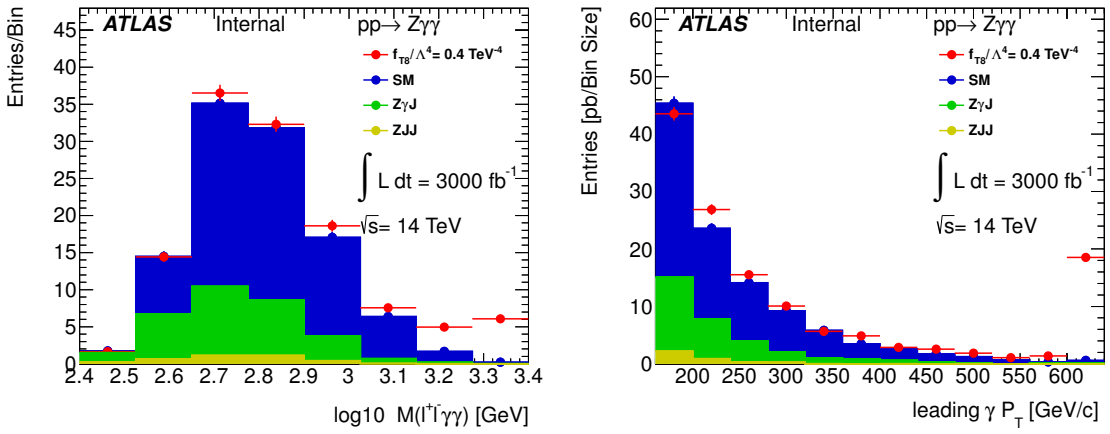

Figure 4: Reconstructed mass spectrum using the charged leptons and photons (left) and leading photon p_T (right) after event selection. The overflow bin is included in the plot. *** ATLAS INTERNAL ***

	5σ 300 fb^{-1}	5σ 3000 fb^{-1}	95% C.I. 300 fb^{-1}	95% C.I. 3000 fb^{-1}
f_{T8}/Λ^4	0.9 TeV^{-4}	0.4 TeV^{-4}	0.5 TeV^{-4}	0.2 TeV^{-4}
f_{T9}/Λ^4	1.8 TeV^{-4}	0.7 TeV^{-4}	1.0 TeV^{-4}	0.4 TeV^{-4}

Table 4: Summary of expected sensitivity to anomalous $Z\gamma\gamma$ production at $\sqrt{s} = 14$ TeV, quoted in the terms of 5σ-significance discovery values and 95% C.I. of f_{T8}/Λ^4 and f_{T9}/Λ^4.

8 Conclusions

Results of sensitivity studies are shown for high-mass ZZ, WZ and $W^\pm W^\pm$ scattering as well as $Z\gamma\gamma$ triboson production using higher dimension operators to parameterize BSM contributions. All heavy gauge bosons are detected in leptonic decay modes. Comparisons of discovery potential are presented for 300 fb^{-1} and 3000 fb^{-1} of integrated luminosity at a pp collision center-of-mass energy of 14 TeV.

We have studied one dimension-6 operator and four dimension-8 operators. Their values for 5σ-significance discovery are summarised in Table 5. The higher integrated luminosity increases the discovery range of these operators' coefficients by more than a factor of two. Optimization of the analyses with 3000 fb^{-1} would lead to further increases in sensitivity. Should new physics parameterized by these operators be discovered with 300 fb^{-1}, the coefficients can be measured with a precision of 5% or better with 3000 fb^{-1} of integrated luminosity, enabling a precision study of this BSM sector.

Parameter	dimension	channel	Λ_{UV} [TeV]	300 fb^{-1}		3000 fb^{-1}	
				5σ	95% CL	5σ	95% CL
$c_{\phi W}/\Lambda^2$	6	ZZ	1.9	33.6 TeV^{-2}	19.5 TeV^{-2}	16.4 TeV^{-2}	9.3 TeV^{-2}
f_{S0}/Λ^4	8	$W^\pm W^\pm$	2.0	10.4 TeV^{-4}	6.8 TeV^{-4}	4.5 TeV^{-4}	0.8 TeV^{-4}
f_{T1}/Λ^4	8	WZ	3.7	1.3 TeV^{-4}	0.7 TeV^{-4}	0.6 TeV^{-4}	0.3 TeV^{-4}
f_{T8}/Λ^4	8	$Z\gamma\gamma$	12.2	0.9 TeV^{-4}	0.5 TeV^{-4}	0.4 TeV^{-4}	0.2 TeV^{-4}
f_{T9}/Λ^4	8	$Z\gamma\gamma$	13.0	2.0 TeV^{-4}	0.9 TeV^{-4}	0.7 TeV^{-4}	0.3 TeV^{-4}

Table 5: 5σ-significance discovery values and 95% CL limits for coefficients of higher-dimension operators. Λ_{UV} is the unitarity violation bound corresponding to the sensitivity with 3000 fb^{-1} of integrated Luminosity. The 95% CL limits are estimated with 1.96σ values.

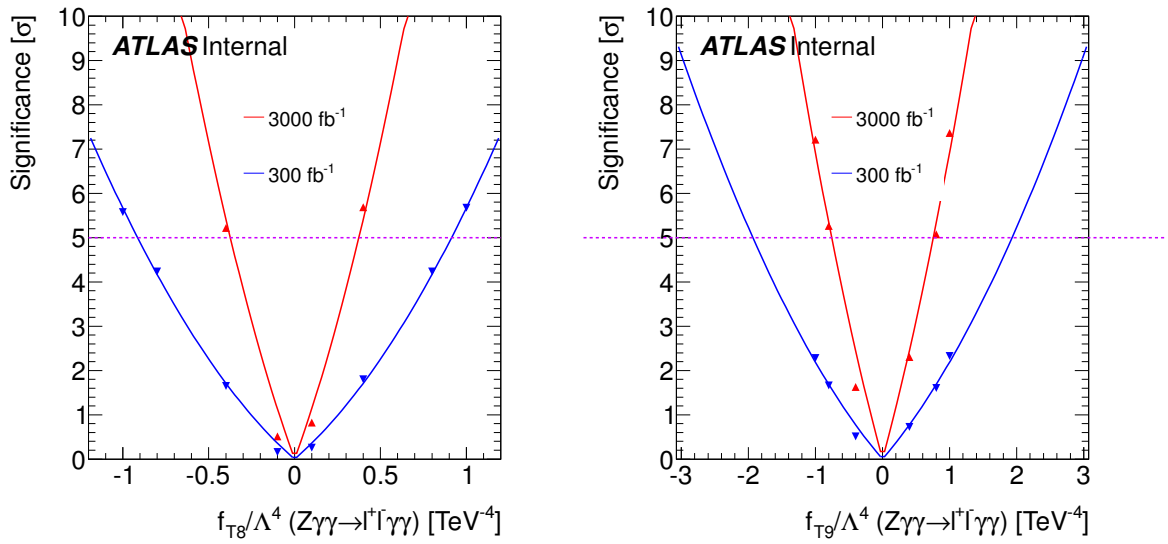

Figure 5: The signal significance as a function of f_{T8}/Λ^4 (left) and f_{T9}/Λ^4 (right). *** ATLAS INTERNAL ***

References

[1] D. Yang, Y. Mao, Q. Li, S. Liu, Z. Xu, et al., *Probing W+W-gamma Production and Anomalous Quartic Gauge Boson Couplings at the CERN LHC*, JHEP **1304** (2013) 108, arXiv:1211.1641 [hep-ph].

[2] C. Degrande, N. Greiner, W. Kilian, O. Mattelaer, H. Mebane, et al., *Effective Field Theory: A Modern Approach to Anomalous Couplings (private communication)*, arXiv:1205.4231 [hep-ph].

[3] O. Eboli, M. Gonzalez-Garcia, and J. Mizukoshi, $pp \to jje^{\pm}\mu^{\pm}\nu\nu$ *and* $jje^{\pm}\mu^{\pm}\nu\nu$ *at* $O(\alpha_{em}^6)$ *and* $O(\alpha_{em}^4\alpha_s^2)$ *for the study of the quartic electroweak gauge boson vertex at CERN LHC*, Phys.Rev. **D74** (2006) 073005, arXiv:hep-ph/0606118 [hep-ph].

[4] T. ATLAS-Collaboration, *Studies of Vector Boson Scattering with an Upgraded ATLAS Detector at a High-Luminosity LHC*, Tech. Rep. ATL-PHYS-PUB-2012-005, CERN, Geneva, Nov, 2012.

[5] http://www.itp.kit.edu/ vbfnloweb/wiki/doku.php?id=download:formfactor.

[6] http://www.itp.kit.edu/prep/diploma/PSFiles/Diplom_Feigl.pdf.

[7] http://www.itp.kit.edu/prep/diploma/PSFiles/Diplom_Schlimpert.pdf.

[8] J. Alwall, M. Herquet, F. Maltoni, O. Mattelaer, and T. Stelzer, *MadGraph 5 : Going Beyond*, JHEP **1106** (2011) 128, arXiv:1106.0522 [hep-ph].

[9] T. Sjostrand, S. Mrenna, and P. Z. Skands, *PYTHIA 6.4 physics and manual*, JHEP **0605** (2006) 026, arXiv:0603175 [hep-ph].

[10] J. Pumplin, D. Stump, J. Huston, H. Lai, P. M. Nadolsky, et al., *New generation of parton distributions with uncertainties from global QCD analysis*, JHEP **0207** (2002) 012, arXiv:hep-ph/0201195 [hep-ph].

[11] M. Cacciari, G. P. Salam, and G. Soyez, *FastJet User Manual*, Eur.Phys.J. **C72** (2012) 1896, arXiv:1111.6097 [hep-ph].

[12] ATLAS Collaboration, *Performance inputs to the 2012 European Strategy studies*, Tech. Rep. ATL-COM-UPGRADE-2012-032, CERN, Geneva, 2012. https://cdsweb.cern.ch/record/1483523.

[13] ATLAS Collaboration, *Physics at a High-Luminosity LHC with ATLAS*, Tech. Rep. ATL-PHYS-PUB-2012-001, CERN, Geneva, Aug, 2012.

[14] S. Ovyn, X. Rouby, and V. Lemaitre, *DELPHES, a framework for fast simulation of a generic collider experiment*, arXiv:0903.2225 [hep-ph].